Research on power distribution control of parallel microgrid based on adaptive capacitor algorithm

Zhanying Tong*

School of Electrical Engineering and Automation,
Henan Institute of Technology,
Xinxiang City, Henan Province, China
Email: zytong20@163.com
*Corresponding author

Liutong Xu

School of Mechanical and Electrical Engineering,
Henan Institute of Science and Technology,
Xinxiang City, Henan Province, China
Email: 17303806905@163.com

Abstract: In order to improve the stability and flexibility of microgrid operation, a droop control strategy for parallel microgrid power distribution based on adaptive virtual capacitor algorithm is proposed. The adaptive virtual capacitor is connected in parallel at the output of microgrid inverter to achieve accurate reactive power sharing of microgrid. The experimental results show that the average power sharing error of distributed generation under the control of adaptive virtual capacitor algorithm is 1.05%, which can effectively realise the accurate power distribution of microgrid and effectively avoid the problem of voltage drop. Add additional load to the system, and the distributed generation tends to be stable within 0.1s after a short transient process. The adaptive virtual capacitor algorithm has good adaptability to load changes, can effectively realise the accurate power distribution of parallel micro grid, and provides a new research idea for the operation optimisation of smart grid.

Keywords: microgrid; virtual capacitance; droop control; reactive power; power sharing.

Reference to this paper should be made as follows: Tong, Z. and Xu, L. (2023) 'Research on power distribution control of parallel microgrid based on adaptive capacitor algorithm', *Int. J. Wireless and Mobile Computing*, Vol. 24, No. 1, pp.17–26.

Biographical notes: Zhanying Tong is a Lecturer with the School of Electrical Engineering and Automation at the Henan Institute of Technology, Xinxiang, China. He received the BS degree from Zhengzhou Institute of Light Industry, China in 2004 and the MS degree in 2009. His research interests include electrical automation, embedded and smart grid technologies.

Liutong Xu is a Master candidate in Henan Institute of Science and Technology. His research interests include surface strengthening and remanufacturing key technologies.

1 Introduction

With the large consumption of traditional fossil energy, energy crisis and environmental problems have attracted extensive attention. The efficient utilisation of clean energy has become the key direction of energy technology development. Among them, the distributed power generation technology of clean power generation has begun to rise and gradually become a key component of intelligent power network (Yang et al., 2019; Liu et al., 2019). Distributed power generation makes centralised use of dispersed clean energy such as wind energy and solar energy in a modular way, so as to enhance the utilisation rate of clean energy, realise energy efficient utilisation, and alleviate the current problems of energy shortage and environmental pollution (Sun et al., 2019; Hashemi et al., 2020). In order to avoid the impact caused by the direct integration of distributed power generation into the power grid and ensure the stability and safety of power grid operation, the way of networking before access is usually adopted for distributed power generation and the way of microgrid system is used to realise the safety and controllability of grid connection (Micallef, 2019; Raza and Jiang, 2019). Microgrid is independent and controllable, which can effectively balance the operation pressure of the power system, enhance the allocation of local energy of the power grid, disconnect from the power grid and enter the island operation state for independent power generation, with high flexibility (Negi et al., 2019). The power distribution of microgrid is directly related to the stable operation of the system and the energy supply of load. If the load difference of

distributed generation is too large, some distributed generation will be overloaded and threaten the stability of the whole microgrid system (Wu et al., 2006; Ni et al., 2019).

For the power distribution control of microgrid, many researchers have proposed a variety of control strategies from different perspectives. In order to solve the problem of voltage deviation caused by line impedance difference in microgrid power distribution, Zhang et al. (2021) proposed an island microgrid power distribution integrated control algorithm based on improved virtual synchronous generator. The microgrid power distribution is controlled through adaptive droop coefficient, the resistance component in line impedance is eliminated and the grid power is adjusted in real-time to improve the distribution accuracy (Zhang et al., 2019). Raza and Jiang (2019) proposed a power control algorithm suitable for the isolated three-phase residential microgrid. The improved vector control and multi-stage (p/f) droop control are used to realise the microgrid power control. The interphase power is transmitted through the converter to realise the interphase and in-phase power control and management. The research results show that the algorithm can effectively realise the power balance of the microgrid and ensure the stable operation of the three-phase residential microgrid (Raza and Jiang, 2019). Yan et al. (2019) proposed a virtual synchronous generator control strategy based on local data to solve the problems of uncontrollable end coefficient and end power coupling of microgrid, and can realise the active power and reactive power distribution control of parallel microgrid in combination with virtual rotor characteristic matching. The research results show that the control strategy has high adaptability and robustness (Yan et al., 2019). Ramezani et al. (2019) proposed the active power and reactive power control of parallel converter based on virtual impedance by analysing the self-impedance and output impedance characteristics of voltage source converter. Starting from the impact of unbalanced impedance on the performance and power of parallel converter, effective power distribution is realised through virtual impedance (Ramezani et al., 2019). From the research results of many researchers, it can be seen that virtual access is a common means to solve the power distribution control of microgrid, but its control accuracy needs to be improved, and it will lead to other negative chain effects. Therefore, the research hopes to solve the limitations of traditional droop control strategy and improve the power distribution accuracy of microgrid by introducing the adaptive virtual capacitor algorithm.

This paper studies the way to increase the adaptive virtual capacitance at the output of the microgrid inverter. Through the adaptive adjustment of the virtual capacitance, the mutual offset singularity of the virtual capacitance and resistance inductance is avoided, the adaptive performance of the microgrid system under different load conditions is enhanced and the power sharing of the microgrid is realised. The droop control of the virtual capacitor is studied to improve the accuracy of reactive power sharing, which effectively solves the problem of voltage amplitude drop caused by the traditional virtual impedance algorithm. While improving the accuracy of reactive power sharing, the output voltage is raised.

The research is mainly carried out from three parts. The first part analyses the reactive power allocation and virtual capacitor characteristics of microgrid, and describes the droop control strategy of parallel microgrid power allocation based on the adaptive virtual capacitor algorithm in detail. The second part is the simulation experiment and analysis of the application effect of the control strategy based on the adaptive virtual capacitor to verify the feasibility and effectiveness of the adaptive virtual capacitor algorithm. The last part is a summary of the whole article.

2 Reactive power distribution control of parallel microgrid based on adaptive virtual capacitor

2.1 Analysis of virtual capacitor and reactive power distribution of microgrid

The reactive power distribution of microgrid is affected by distributed generation, users, load and other factors. Its output impedance and line impedance may not meet the conditions of accurate reactive power sharing, and it is prone to reactive power sharing error (Hoang and Lee, 2020; Shen et al., 2020). Moreover, the average error of reactive power is also affected by the droop coefficient of distributed generation and the voltage at the common connection point, and the reactive load has an important impact on the voltage at the common connection point. Therefore, the average error of reactive power in microgrid is also related to the change of load reactive power (Jia et al., 2019; Liu et al., 2019). Therefore, in order to realise the reactive power sharing of microgrid, it is necessary to comprehensively consider three factors: line impedance, output impedance and sag coefficient. The output reactive power difference of parallel microgrid has a positive correlation with the line impedance ratio and reactive load, and a negative correlation with the sag coefficient. Therefore, reducing the line impedance difference and increasing the reactive sag coefficient are the two main means to realise the equal distribution of reactive power in microgrid (Phurailatpam et al., 2019; Shahid et al., 2019). Virtual impedance is a common way to realise microgrid power decoupling control. The inductive reactance component is changed by virtual impedance control algorithm to improve the accuracy of microgrid power sharing (Firdaus, 2020). However, there are some limitations in the way of virtual impedance. While the averaging accuracy is improved, the voltage amplitude of microgrid drops (Vergara et al., 2019). Therefore, based on the principle of virtual impedance algorithm, the research adjusts the reactive power and voltage amplitude of microgrid by adding adaptive virtual capacitor at the output of inverter, improves the accuracy of reactive power sharing of microgrid and raises the output voltage to avoid the problem of voltage amplitude drop.

Figure 1 Equivalent circuit of parallel inverter

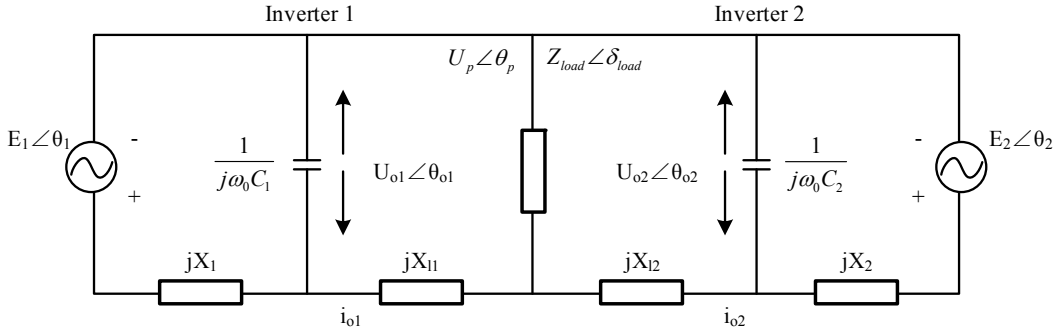

To facilitate the analysis, take the parallel system of two inverters as an example to analyse the reactive power output of microgrid after adding capacitors. The equivalent circuit of parallel inverter is shown in Figure 1. The equivalent circuit of parallel inverter is composed of two distributed power interface inverters, including voltage source, output impedance, line impedance, common load and capacitance. An ideal voltage source and output impedance are used to replace the inverter structure, in which the line impedance and output impedance of the inverter are inductive. Where $E_i\angle\theta_i$ is the voltage of the voltage source, jX_i is the output impedance, jX_{li} is the line impedance, the voltage value and impedance value of the common load are $U_p\angle\theta_p$ and $Z_{load}\angle\delta_{load}$, respectively, θ represents the voltage phase angle, E represents the inverter output voltage amplitude, U represents the common load voltage amplitude, Z represents the common load impedance, and δ represents the phase voltage phase angle. The output voltage function of inverter 1 before and after adding capacitance is shown as follows:

$$\begin{cases} U_{o1}\angle\theta_{o1} = \dfrac{X_{l1}E_1\angle\theta_1 + X_1U_P\angle\theta_P}{X_{l1}+X_1} \\ U_{o1c}\angle\theta_{o1c} = \dfrac{X_{l1}E_1\angle\theta_1 + X_1U_P\angle\theta_P}{X_{l1}+X_1-\omega_0C_1X_{l1}X_1} \end{cases} \tag{1}$$

In equation (1), $U_{o1}\angle\theta_{o1}$ represents the output voltage of inverter 1 before the shunt capacitor, $U_{o1c}\angle\theta_{o1c}$ represents the output voltage of inverter 1 after the shunt capacitor, X_{l1} represents the line impedance inductive component of inverter 1, $E_1\angle\theta_1$ represents the voltage value of inverter 1, X_1 represents the output impedance inductive component of inverter 1, ω_0 represents the rated angular frequency of voltage and C_1 represents the capacitance of inverter 1 in parallel. The output voltage function of inverter 2 before and after adding capacitance is expressed as follows:

$$\begin{cases} U_{o2}\angle\theta_{o2} = \dfrac{X_{l2}E_2\angle\theta_2 + X_2U_P\angle\theta_P}{X_{l2}+X_2} \\ U_{o2c}\angle\theta_{o2c} = \dfrac{X_{l2}E_2\angle\theta_2 + X_2U_P\angle\theta_P}{X_{l2}+X_2-\omega_0C_2X_{l2}X_2} \end{cases} \tag{2}$$

In equation (2), $U_{o2}\angle\theta_{o2}$ represents the output voltage of inverter 2 before the parallel capacitor, $U_{o2c}\angle\theta_{o2c}$ represents the output voltage of inverter 2 after the parallel capacitor, X_{l2} represents the line impedance inductive component of inverter 2, $E_2\angle\theta_2$ represents the voltage value of inverter 2, X_2 represents the output impedance inductive component of inverter 2 and C_2 represents the capacitance of inverter 2 in parallel. After the virtual capacitor is added, the output voltage of inverter 1 and inverter 2 subtracts the virtual capacitor value from the line impedance and the inductive component of output impedance, so that the output voltage of inverter increases. The values of phase angles θ_1, θ_2 and θ_p are small, and the value relationship is shown as follows:

$$\begin{cases} \cos\theta_1 = \cos\theta_2 = \cos\theta_p = 1 \\ \sin\theta_1 = \sin\theta_2 = \sin\theta_p = 0 \end{cases} \tag{3}$$

Substitute equation (3) into equations (1) and (2), the output voltage function of inverter 1 and inverter 2 before and after adding capacitance can be expressed as follows:

$$\begin{cases} U_{o1} = \dfrac{X_{l1}E_1 + X_1U_P}{X_{l1}+X_1} \\ U_{o1c} = \dfrac{X_{l1}E_1 + X_1U_P}{X_{l1}+X_1-\omega_0C_1X_{l1}X_1} \\ U_{o2} = \dfrac{X_{l2}E_2 + X_2U_P}{X_{l2}+X_2} \\ U_{o2c} = \dfrac{X_{l2}E_2 + X_2U_P}{X_{l2}+X_2-\omega_0C_2X_{l2}X_2} \end{cases} \tag{4}$$

The output voltages U_{o1} and U_{o2} of the two inverters before adding capacitors are compared with the output voltages U_{o1c} and U_{o2c} after adding capacitors. After adding capacitors at the inverter output end, the virtual capacitance value is subtracted from the inverter line impedance and output impedance. Using virtual capacitors to adjust the inverter line impedance and output impedance can effectively increase the inverter output voltage value. The output voltage value is positively correlated with the capacitance value. The reactive power of inverter 1 and inverter 2 before adding capacitor is shown as follows:

$$\begin{cases} Q_{o1} \approx \dfrac{U_p\left(E^* - U_p\right)}{n_1 U_p + X_1 + X_{l1}} \\ Q_{o2} \approx \dfrac{U_p\left(E^* - U_p\right)}{n_2 U_p + X_2 + X_{l2}} \end{cases} \tag{5}$$

In equation (5), Q_{o1} represents the reactive power of the output end of inverter 1 before the shunt capacitor, Q_{o2} represents the reactive power of the output end of inverter 2 before the shunt capacitor, E^* represents the rated voltage value of the output end of inverter and n_1 and n_2 represent the reactive droop coefficients of inverter 1 and inverter 2, respectively. After the virtual capacitor is connected in parallel on the inverter, the virtual capacitor value is added to the rated voltage value at the output end of the inverter, and the virtual capacitor value is subtracted from the output impedance, line impedance and common load to increase the output reactive power of the inverter. The reactive power of inverter 1 and inverter 2 after adding capacitors is shown as follows:

$$\begin{cases} Q_{o1c} = \dfrac{U_p\left(E^* + \omega_0 C_1 X_1 U_p - U_p\right)}{n_1 U_p + X_1 + X_{l1} - \omega_0 C_1 X_1 X_{l1}} \\ Q_{o2c} = \dfrac{U_p\left(E^* + \omega_0 C_2 X_2 U_p - U_p\right)}{n_2 U_p + X_2 + X_{l2} - \omega_0 C_2 X_2 X_{l2}} \end{cases} \tag{6}$$

In equation (6), Q_{o1c} represents the reactive power of the output end of inverter 1 after the shunt capacitor, and Q_{o2c} represents the reactive power of the output end of inverter 2 after the shunt capacitor. Among them, $\omega_0 C_i X_i X_{li} \ll X_i + X_{li}$ and $\omega_0 C_i X_i X_{li}$ can be ignored. The simplified function of reactive power of inverter 1 and inverter 2 after adding capacitance is expressed as follows:

$$\begin{cases} Q_{o1c} = Q_{o1} + \dfrac{\omega_0 X_1 U_p^2}{n_1 U_p + X_1 + X_{l1}} C_1 \\ Q_{o2c} = Q_{o2} + \dfrac{\omega_0 X_2 U_p^2}{n_2 U_p + X_2 + X_{l2}} C_2 \end{cases} \tag{7}$$

The output reactive power can be effectively increased by paralleling the capacitor at the output of the inverter, and the reactive power is positively correlated with the value of the shunt capacitor. After adding a capacitor at the output end of the inverter, the function of reactive power distribution difference ΔQ is expressed as follows:

$$\Delta Q = n_1 Q_{o1} - n_2 Q_{o2} + \omega_0 U_p^2 \left(\frac{n_1 C_1 X_1}{n_1 U_p + X_{l1} + X_1} - \frac{n_2 C_2 X_2}{n_2 U_p + X_{l2} + X_2} \right) \tag{8}$$

By comparing the reactive power of inverter 1 and inverter 2 before and after adding capacitors, it can be seen that adding capacitors at the output end of the inverter can effectively adjust the reactive power of the inverter by adjusting capacitors C_1 and C_2. The relationship between the inverter reactive power and the capacitor meets the droop. By establishing the droop control formula to control the size of capacitors C_1 and C_2, the inverter reactive power distribution can be effectively and accurately controlled. When $n_2\left(X_{l1} + X_1\right) > n_1\left(X_{l2} + X_2\right)$, $n_2 Q_{o2} > n_1 Q_{o1}$, the reactive power sharing error of the inverter can be reduced by adjusting the size of capacitors C_1 and C_2 to $n_2 X_2 C_2 > n_1 X_1 C_1$. When $n_2\left(X_{l1} + X_1\right) < n_1\left(X_{l2} + X_2\right)$, $n_2 Q_{o2} < n_1 Q_{o1}$, the reactive power sharing error of the inverter can be reduced by adjusting the size of capacitors C_1 and C_2 to $n_2 X_2 C_2 < n_1 X_1 C_1$.

2.2 Droop control strategy based on adaptive virtual capacitor

Based on the virtual capacitor, the virtual capacitor algorithm is used to adjust the voltage amplitude and reactive power of the microgrid, so as to enhance the accuracy of reactive power sharing in the microgrid. The adaptive virtual capacitor operator is introduced into the algorithm for adaptive improvement and optimisation. Through the adaptive adjustment of the virtual capacitor, the offset singularity of the virtual capacitor and resistance is avoided, and the power sharing is realised. Firstly, the virtual capacitor algorithm is used to control the reactive power distribution of the microgrid. The virtual capacitor algorithm simulates the capacitor characteristics in the form of the control algorithm. The virtual capacitor is connected in parallel at the output of the inverter to achieve accurate adjustment of reactive power and amplitude. Adding a physical capacitor directly to the inverter output will increase the equipment volume, increase the economic cost of the microgrid system, and it is difficult to realise the continuous real-time adjustment of the capacitance value of the physical capacitor. The virtual capacitor method can effectively avoid the problems caused by the physical capacitor (Sepehrzad et al., 2020; Razi et al., 2020). The relationship among output voltage $U_{o1}\angle\theta_{o1}$, voltage value $E_1\angle\theta_1$ and output current i_{o1} of inverter 1 before shunt capacitor meets the equation:

$$U_{o1}\angle\theta_{o1} = E_1\angle\theta_1 + X_1\omega_0 C_1 U_{o1}\angle\theta_{o1} - jX_1 i_{o1} \tag{9}$$

The voltage closed-loop reference voltage $E_{1c}\angle\theta_{1c}$ function after the inverter is connected in parallel with the virtual capacitor is expressed as follows:

$$E_{ic}\angle\theta_{ic} = E_i\angle\theta_i + \omega_0 X_i C_i U_{oi}\angle\theta_{oi} \tag{10}$$

Since phase angles θ_1 and θ_2 are small, their values meet the following conditions:

$$\begin{cases} \cos\theta_1 = \cos\theta_2 = 1 \\ \sin\theta_1 = \sin\theta_2 = 0 \end{cases} \tag{11}$$

The Virtual Capacitance algorithm function can be expressed as follows:

$$E_{ic} = E_i + \omega_0 X_i C_i U_{oi} \tag{12}$$

The algorithm block diagram of the Virtual Capacitance algorithm is shown in Figure 2. The Virtual Capacitance algorithm uses the control algorithm to simulate the capacitance data. On the basis of keeping the original volume of the equipment unchanged, the virtual capacitance is added at the output end of the inverter and the Virtual Capacitance $\omega_0 X_i C_i U_{oi}$ is introduced into the output reference voltage E_i of the original power outer ring to realise the effective adjustment of reactive power sharing.

Figure 2 Block diagram of virtual capacitance algorithm

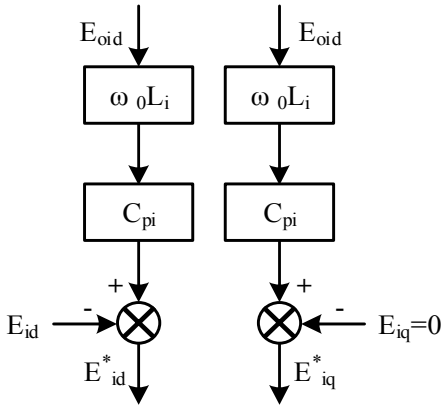

The reactive power sharing condition function of inverter 1 and inverter 2 after adding virtual capacitor is expressed as follows:

$$\begin{cases} U_{o1c} = \dfrac{n_2}{n_1 + n_2} Q_{load} \\ U_{o2c} = \dfrac{n_1}{n_1 + n_2} Q_{load} \end{cases} \tag{13}$$

In equation (13), Q_{load} represents load power. Combined with the reactive power function of the inverter, the Virtual Capacitance function of the inverter in parallel can be expressed as follows:

$$\begin{cases} C_1 = \left(\dfrac{n_2}{n_1 + n_2} Q_{load} - Q_{o1} \right) / t_1 \\ C_2 = \left(\dfrac{n_1}{n_1 + n_2} Q_{load} - Q_{o2} \right) / t_2 \end{cases} \tag{14}$$

In equation (14), t_1 and t_2 represent the transmission time. The function t_i is expressed as follows:

$$t_i = \frac{\omega_0 X_i U_p^2}{n_1 U_p + X_i + X_{li}} \tag{15}$$

It can be seen from equation (15) that the accurate sharing of reactive power is related to the line impedance, output impedance, sag coefficient, total load power and other parameter values. The cost of microgrid system will be increased by using communication transmission, and the control of communication transmission is difficult. In case of communication failure, data reception may be delayed. It affects the control algorithm and the normal and stable operation of microgrid system. Combined with the droop relationship between microgrid reactive power and virtual capacitance, the Virtual Capacitance function is expressed as follows:

$$\begin{cases} C_1 = C_1^* - k_{c1} Q_{o1} \\ C_2 = C_2^* - k_{c2} Q_{o2} \end{cases} \tag{16}$$

In equation (16), C_1^* and C_2^*, respectively represent the maximum Virtual Capacitance of inverter 1 and inverter 2 when $Q_{oi} = 0$, and k_{c1} and k_{c2} are the Virtual Capacitance droop coefficients. When $Q_{oi} = 0$, the Virtual Capacitance algorithm function is expressed as follows:

$$E_{ic} \Big|_{Q_{oi}=0} \approx E^* + \omega_0 X_i C_i^* E^* \le E_{\max} \tag{17}$$

In equation (17), $E_{\max}$ represents the maximum voltage amplitude of the system. The maximum virtual capacitance value function is expressed as follows:

$$C_i^* = \frac{E_{\max} - E_i^*}{\omega_0 X_i E_i^*} = \frac{n_i Q_{irate}}{\omega_0 X_i E_i^*} \tag{18}$$

In equation (18), Q_{irate} represents the power ratio. In order to avoid the voltage drop problem of inductive component load, the constraint conditions of virtual capacitance value are shown as follows:

$$C_{i\min} \Big|_{Q_{oi}=Q_{irate}} \approx C_i^* - k_{ci} Q_{irate} \ge 0 \tag{19}$$

The constraint conditions of Virtual Capacitance sag coefficient are expressed as follows:

$$\begin{cases} k_{ci} = \dfrac{n_i}{\omega_0 X_i E_i^*} \le \dfrac{C_i^*}{Q_{irate}} \\ 0 < n_i \le 1 \end{cases} \tag{20}$$

Combined with the virtual capacitance value and various constraints, the Virtual Capacitance algorithm function is expressed as follows:

$$E_{ic} = E_i + \omega_0 X_i C_i U_{oi} = E_i + \frac{n_i U_{oi}}{E_i^*} \left(Q_{irate} - Q_i \right) \tag{21}$$

The Virtual Capacitance algorithm realises the accurate sharing of reactive power of microgrid by adjusting the reactive power and voltage amplitude without the action of communication transmission and other parameters. The algorithm has simple operation and strong applicability (Akhtar et al., 2019; Jayachandran and Ravi, 2019). However, when the system load is resistive, there is a problem that the phase angle of the load resistive and the Virtual Capacitance offset, resulting in the load showing resistance characteristics (Sabir and Javaid, 2019; Wenjuan et al., 2019). The Virtual Capacitance algorithm has specific load specific points in the control process, resulting in the microgrid system cannot achieve power sharing under arbitrary load changes. Therefore, it is necessary to adaptively improve and optimise

the Virtual Capacitance algorithm (Wu et al., 2019; Liu et al., 2020). The adaptive virtual capacitor is used to avoid the offset singularity, improve the accuracy of reactive power sharing of microgrid, so as to realise the 'plug and play' of distributed power generation, enhance the adaptability of microgrid system to different load conditions and ensure the control effect of microgrid system in the face of sudden load changes. The virtual capacitance of microgrid inverter in parallel is used to change the load impedance angle, and the virtual capacitance is regarded as a component of the load, so as to eliminate the influence of load state change on the power sharing accuracy of microgrid. The constraints of the adaptive virtual capacitance operator are expressed as follows:

$$C_i < -\left(n_i - 2\right)Q_i / \left[\left(n_i - 1\right)\omega_0 U_i^2\right] \tag{22}$$

When the Virtual Capacitance operator satisfies equation (22), the existence of a specific load can be avoided. The Virtual Capacitance algorithm adjusts the virtual capacitance to achieve accurate power sharing of the microgrid. The virtual capacitance has a positive correlation with the reactive power of the microgrid. Therefore, the coefficient of the virtual capacitance is a small value, which can effectively realise the adaptation of the virtual capacitance and the system load. The adaptive virtual capacitance function is expressed as follows:

$$C_i = m\left|Q_i\right| = 1/\left(\omega_0 U_i^2\right)\left|Q_i\right| \tag{23}$$

In equation (23), m is the Virtual Capacitance coefficient. If the added virtual capacitance is too large, it may affect the operation stability of the microgrid system. Therefore, the reactive power of the microgrid needs to be kept within a certain range. When $-Q_{\min} \le Q_i \le Q_{\min}$, $Q_{\min}$ represents the minimum reactive power of the microgrid, and the initial value of the added virtual capacitance, while $Q_{\min}$ is generally about 0.01 times the load reactive power. At this time, the parallel virtual capacitance is small, it will not have a negative impact on the stability of microgrid system.

2 Simulation experiment and result analysis

In order to verify the effectiveness and feasibility of the virtual capacitor algorithm in the power distribution of parallel microgrid, a microgrid simulation model is built by using the MATLAB simulation platform. Two distributed generators are connected in parallel to form a parallel inverter line. The data parameters of the microgrid simulation model under the parallel connection of two distributed generators are shown in Table 1.

The two distributed generators adopt the traditional P-F / q-u droop control mode in the stage of 0–0.5 s, and take 0.5 s as the switching time point to convert the control strategy into the droop control mode based on the virtual capacitor algorithm. The total simulation time is set to 1 s. The output reactive power and output voltage of the two distributed generators are shown in Figure 3.

Table 1 Simulation parameters of parallel microgrid

Parameter	*Numerical value*
Rated output voltage	*E**=311 V
Load	*Q*=3000 Var
Distributed power capacity	Q1rate=Q1rate=2000 Var
Line impedance	*X*l1=*X*l2=1.5×10–3H
Sag coefficient	*n*=7.775×10–3
Voltage loop parameters	*Kp*=10, *Ki*=100
Current loop parameters	*K*=2
Filter parameters	*L*=0.6 mH, *C*=150 μF

As can be seen from Figure 3, in the first 0.5 s, the traditional P-F / q-u droop control strategy is used for microgrid reactive power distribution. The output reactive power of distributed power supply 1 and distributed power supply 2 is 1850 var and 1000 var, respectively, and the output voltage of distributed power supply 1 and distributed power supply 2 is 295 V, Under the traditional P-F / q-u droop control, the difference of output reactive power between distributed generation 1 and distributed generation 2 is 850 var. After 0.5 s, the virtual capacitor algorithm is used for power distribution. The output reactive power of distributed generation 1 and distributed generation 2 is 1600 var and 1350 var, respectively, and the output voltage of distributed generation 1 and distributed generation 2 is 300 V. Under the control of virtual capacitor algorithm, the difference of output reactive power between distributed generation 1 and distributed generation 2 is 250 var, which is reduced by 600 var compared with traditional P-F / q-u droop control, and the difference of output reactive power of microgrid is reduced by 70.59%. It is proved that virtual capacitor algorithm can effectively improve the accuracy of reactive power sharing of parallel microgrid. After the virtual capacitor is added, the output voltage of distributed generation 1 and distributed generation 2 is increased by 5 V, which proves that the virtual capacitor algorithm can effectively raise the output voltage of microgrid and avoid the problem of voltage drop.

In order to verify the optimisation of the adaptive virtual capacitor algorithm, compare the control effect of the virtual capacitor algorithm and the adaptive virtual capacitor algorithm when facing the increase of load impedance. Take 1 s as the load switching time point, and after 1 s, add a constant power load with active power of 4000 W and reactive power of 5000 var into the microgrid system. The simulation experiment time is 2 s in total, and repeat the experiment for 10 times, The average changes of the output reactive power and output voltage of the distributed power supply are shown in Figure 4. Figures 4(a) and 4(b) show the output power and output voltage of the distributed power supply under the control of the Virtual Capacitance algorithm, and Figures 4(c) and 4(d) show the output power and output voltage of the distributed power supply under the control of the adaptive virtual capacitance algorithm.

Figure 3 Comparison of output reactive power and output voltage of two distributed generators

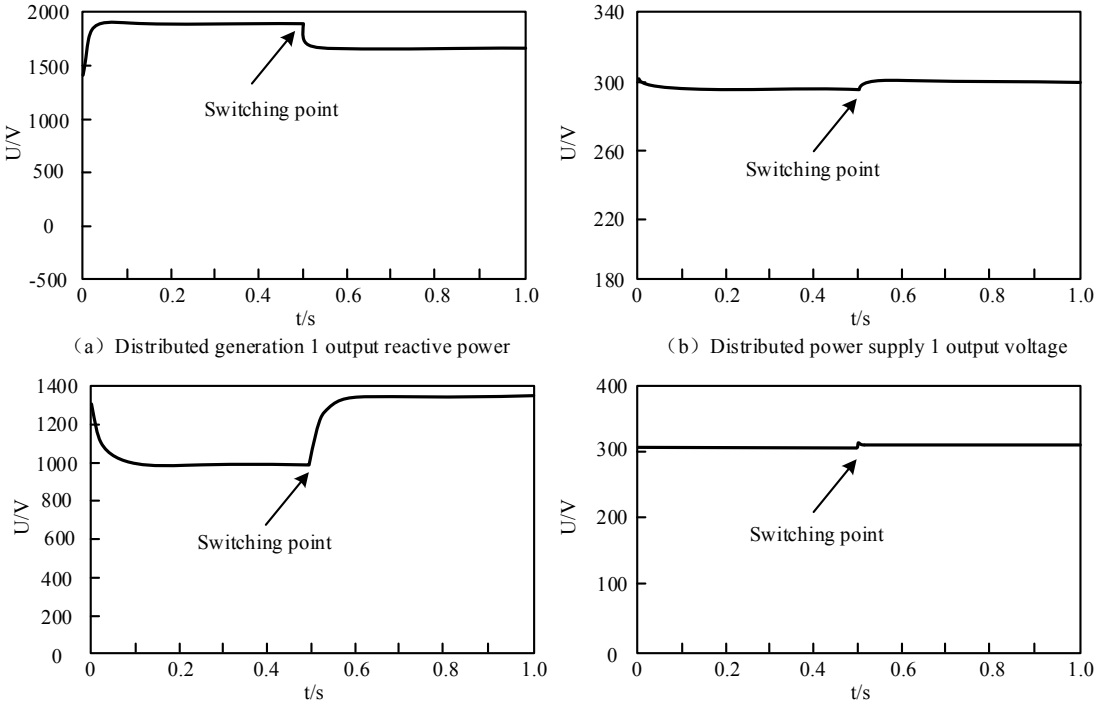

（a）Distributed generation 1 output reactive power

（b）Distributed power supply 1 output voltage

（c）Distributed generation 2 output reactive power

（d）Distributed power supply 2 output voltage

Figure 4 Output reactive power and output voltage of distributed generation under two algorithms

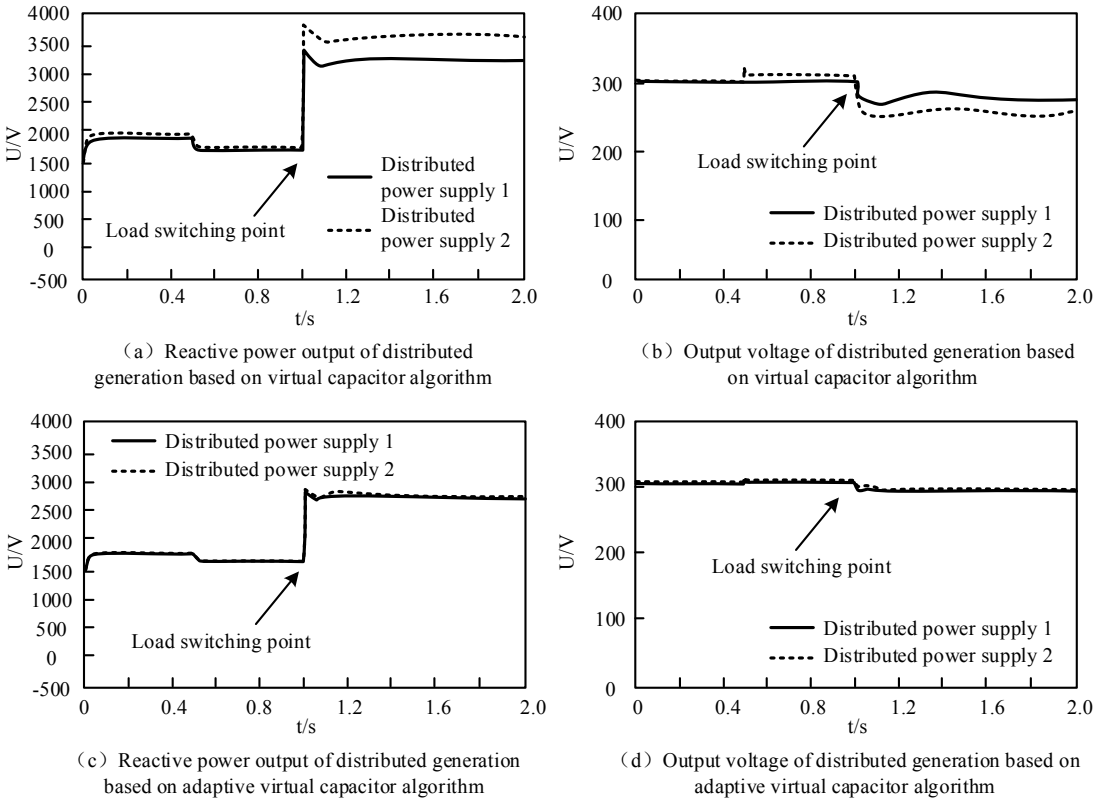

（a）Reactive power output of distributed generation based on virtual capacitor algorithm

（b）Output voltage of distributed generation based on virtual capacitor algorithm

（c）Reactive power output of distributed generation based on adaptive virtual capacitor algorithm

（d）Output voltage of distributed generation based on adaptive virtual capacitor algorithm

Table 2 Model power sharing error under five control modes

Experiment serial number	*Do not introduce virtual access*	*Virtual impedance*	*Virtual inductance*	*Virtual capacitance*	*Adaptive virtual capacitor*
1	3.88%	3.06%	2.77%	1.84%	1.04%
2	3.94%	3.11%	2.65%	1.75%	1.12%
3	3.95%	3.08%	2.71%	1.63%	1.06%
4	3.81%	3.06%	2.69%	1.72%	1.07%
5	3.79%	3.14%	2.79%	1.81%	1.06%
6	3.86%	3.12%	2.78%	1.72%	1.01%
7	3.72%	3.03%	2.74%	1.84%	0.99%
Average error	3.85%	3.09%	2.73%	1.76%	1.05%

As can be seen from Figure 4(a), the average output reactive power of distributed power 1 and distributed power 2 before the increase of additional load is 1967 var and 2000 var, respectively, with a difference of 33 var. After adding additional load, the average output reactive power of distributed power 1 and distributed power 2 is 3400 var and 3700 var, respectively, with a difference of 300 var. Compared with the original load difference, the increase of 267 var will lead to the decrease of reactive power sharing accuracy of microgrid. As can be seen from Figure 4(b), before and after the load increase, the average output voltage difference between distributed power supply 1 and distributed power supply 2 is 5 V and 10 V, respectively. The increase of load increases the voltage drop amplitude of the microgrid and affects the operation stability of the microgrid. It can be seen from Figures 4(c) and 4(d) that the adaptive virtual capacitor algorithm is used for power distribution control. The average output reactive power of distributed power 1 and distributed power 2 is 1681 var and 1700 var, respectively, and the average output voltage of distributed power 1 and distributed power 2 is 300 V. It is proved that the adaptive virtual capacitor algorithm can effectively realise the reactive power sharing of microgrid. After adding additional load, distributed power 1 and distributed power 2 have a short transient process, but they tend to be stable within 0.1s, the output reactive power is stable at 2800var, and the output voltage is maintained at 291 v. It is proved that the adaptive virtual capacitor algorithm can better adapt to sudden load impedance changes, and the operation stability is good. The adaptive virtual capacitor algorithm can effectively solve the negative impact caused by the increase of load impedance, and effectively avoid the reduction of reactive power sharing accuracy caused by the increase of load impedance. Through the adaptive adjustment of virtual capacitor, the precise reactive power sharing of microgrid under the change of load impedance can be realised.

In order to verify the effectiveness and optimisation of the adaptive virtual capacitance algorithm, the application effects without introducing virtual access, virtual impedance algorithm, virtual inductance algorithm, Virtual Capacitance algorithm and adaptive virtual capacitance algorithm are compared and analysed. Seven groups of simulation experiments are carried out for five control modes, and each group of experiments is repeated for 10 times. The power sharing error of the model under the five control modes is shown in Table 2.

As can be seen from Table 2, the average power sharing error of the adaptive virtual capacitance algorithm is 1.05%, which is reduced by 2.04%, 1.68% and 0.71%, respectively compared with the virtual impedance algorithm, the virtual inductance algorithm and the Virtual Capacitance algorithm. It is proved that the adaptive virtual capacitance algorithm can effectively improve the power sharing accuracy of the microgrid system, which is better than the virtual impedance and virtual inductance access mode. The adaptive regulation of the virtual capacitor can effectively improve the load adaptability of the microgrid system, avoid the problem of decreasing the average accuracy due to the increase of load impedance and improve the adaptive control performance of the microgrid system for load fluctuations.

3 Conclusion

In order to ensure the safe and stable operation of microgrid, a droop control strategy for parallel microgrid power distribution based on adaptive virtual capacitor algorithm is proposed. Combined with the structural characteristics of parallel microgrid, the reactive power sharing accuracy of microgrid is improved by paralleling virtual capacitors at the output of microgrid inverter, and the virtual capacitor operator is adaptively improved. In order to improve the response ability of the microgrid to changes in load characteristics and enhance the operation stability of the microgrid system. The experimental results show that compared with the traditional p-f/q-u droop control, the difference of reactive power output of micro grid under the control of virtual capacitor algorithm is reduced by 70.59%. The virtual capacitor algorithm can effectively improve the reactive power sharing accuracy of parallel microgrid, and the addition of virtual capacitor increases the output voltage of microgrid by 5 V, effectively avoiding the problem of voltage drop. The average power sharing error rate of the adaptive virtual capacitor algorithm is 1.05%, which is significantly lower than 3.09% of the virtual impedance algorithm and 2.73% of the virtual inductance algorithm. After the additional load is added, the distributed generation tends to be stable within 0.1 s after a short transient process. The

adaptive virtual capacitor algorithm has good adaptability to load changes and can effectively solve the problem of power sharing accuracy reduction caused by load changes. The research mainly focuses on the research and analysis of the isolated microgrid. In the future, the power distribution of the grid connected microgrid can be taken as the next research direction to improve the comprehensive distribution capacity of the microgrid.

Acknowledgement

This work is supported by: 1. Key Scientific Research Project of Higher Education of Henan Province, Research on Charging and Discharging Measurement and Control System of Lithium Battery Pack for Electric Vehicle (No.16A470019). 2. Key scientific and technological projects in Henan Province in 2022, Research on online information monitoring technology of power cable accessories based on multi physical field coupling (No.222102220102). 3. Key Scientific Research Project of Higher Education of Henan Province, Research on control strategy and energy consumption optimisation of refrigeration system of new energy refrigerator truck (No.22B480002).

References

Akhtar, I., Kirmani, S. and Jamil, M. (2019) 'Analysis and design of a sustainable microgrid primarily powered by renewable energy sources with dynamic performance improvement', *International Journal of IET Renewable Power Generation*, Vol. 13, No. 7, pp.1024–1036.

Firdaus, A. (2020) 'Dynamic power flow based simplified transfer function model to study instability of low-frequency modes in inverter-based microgrids', *International Journal of IET Generation Transmission and Distribution*, Vol. 14, No. 23, pp.5634–5645.

Hashemi, S.M., Vahidinasab, V. and Ghazizadeh, M.S. et al. (2020) 'Load control mechanism for operation of microgrids in contingency state', *International Journal of IET Generation Transmission and Distribution*, Vol. 14, No. 23, pp.5407–5417.

Hoang, K.D. and Lee, H.H. (2020) 'State of charge balancing for distributed battery units based on adaptive virtual power rating in a DC microgrid', *International Journal of Journal of Electrical Engineering and Technology*, Vol. 15, No. 5, pp.2121–2131.

Jayachandran, M. and Ravi, G. (2019) 'Decentralized model predictive hierarchical control strategy for islanded AC microgrids', *International Journal of Electric Power Systems Research*, Vol. 170, pp.92–100.

Jia, L., Miura, Y. and Ise, T. (2019) 'Cost-function-based microgrid decentralized control of unbalance and harmonics for simultaneous bus voltage compensation and current sharing', *International Journal of IEEE Transactions on Power Electronics*, Vol. 34, No. 8, pp.7397–7410.

Liu, B., Liu, Z. and Liu, J. et al. (2019) 'An adaptive virtual impedance control scheme based on small-ac-signal injection for unbalanced and harmonic power sharing in islanded microgrids', *International Journal of IEEE Transactions on Power Electronics*, Vol. 34, No. 12, pp.12333–12355.

Liu, B., Liu, Z. and Liu, J.G. (2020) 'A noninvasive feeder impedance estimation method for parallel inverters in microgrid based on load harmonic current', *International Journal of IEEE Transactions on Power Electronics*, Vol. 36, No. 7, pp.7354–7359.

Liu, W., Gu, W. and Sheng, W. et al. (2019) 'Virtual cluster control for active distribution system using Pinning-based distributed secondary control', *International Journal of International Journal of Electrical Power and Energy Systems*, Vol. 109, pp.710–718.

Micallef, A. (2019) 'Review of the current challenges and methods to mitigate power quality issues in single-phase microgrids', *International Journal of IET Generation, Transmission and Distribution*, Vol. 13, No. 11, pp.2044–2054.

Negi, N., Sahoo, S.R. and Chakrabarti, S. (2019) 'Distributed control based power sharing strategy for an islanded AC microgrid', *International Journal of IET Generation, Transmission, Distribution*, Vol. 13, No. 4, pp.553–562.

Ni, F., Yan, L. and Liu, J. et al. (2019) 'Fuzzy logic-based virtual capacitor adaptive control for multiple HESSs in a DC microgrid system', *International Journal of Electrical Power and Energy Systems*, Vol. 107, pp.78–88.

Phurailatpam, C., Rather, Z.H. and Bahrani, B. et al. (2019) 'Measurement based estimation of inertia in AC microgrids', *International Journal of IEEE Transactions on Sustainable Energy*, Vol. 11, No. 3, pp.1975–1984.

Ramezani, M., Li, S. and Sun, Y (2019) 'DQ-reference-frame based impedance and power control design of islanded parallel voltage source converters for integration of distributed energy resources', *International Journal of Electric Power Systems Research*, Vol. 168, pp.67–80.

Raza, S.A. and Jiang, J. (2019) 'Intra- and inter-phase power management and control of a residential microgrid at the distribution level', *International Journal of IEEE Transactions on Smart Grid*, Vol. 10, No. 6, pp.6839–6848.

Raza, S.A. and Jiang, J. (2019) 'Intra- and inter-phase power management and control of a residential microgrid at the distribution level', *International Journal of IEEE Transactions on Smart Grid*, Vol. 10, No. 6, pp.6839–6848.

Razi, R., Iman-Eini, H. and Hamzeh, M. et al. (2020) 'A novel extended impedance-power droop for accurate active and reactive power sharing in a multi-bus microgrid with complex impedances', *International Journal of IEEE Transactions on Smart Grid*, Vol. 11, No. 5, pp.3795–3804.

Sabir, A. and Javaid, M.S. (2019) 'Minimizing neutral currents in distribution microgrids using smart loads', *International Journal of Electrical Power and Energy Systems*, Vol. 113, pp.436–448.

Sepehrzad, R., Moridi, A.R. and Hassanzadeh, M.E. et al. (2020) 'Energy management and optimal multi-objective power control in AC/DC micro-grid using hybrid energy storage system', *International Journal of Ad Hoc and Ubiquitous Computing*, Vol. 112, No. 1, pp.199–213.

Shahid, M.U., Khan, M.M. and Hashmi, K. et al. (2019) 'Renewable energy source (RES) based Islanded DC microgrid with enhanced resilient control', *International Journal of International Journal of Electrical Power and Energy Systems*, Vol. 113, pp.461–471.

Shen, L., Cheng, Q. and Cheng, Y. et al. (2020) 'Hierarchical control of DC micro-grid for photovoltaic EV charging station based on flywheel and battery energy storage system', *International Journal of Electric Power Systems Research*, Vol. 179, pp.106079.1–106079.11.

Sun, W., Zhao, C. and Wang, J. et al. (2019) 'Distributed cooperative secondary networked optimal control with packet loss for islanded microgrid', *International Journal of IET Generation, Transmission and Distribution*, Vol. 13, No. 20, pp.4733–4740.

Vergara, P.P., Rey, J.M. and López, J.C. et al. (2019) 'A generalized model for the optimal operation of microgrids in grid-connected and islanded droop-based mode', *International Journal of IEEE Transactions on Smart Grid*, Vol. 10, No. 5, pp.5032–5045.

Wenjuan, D.U. and Zheng, K. and Wang, H. (2019) 'Oscillation instability of a DC microgrid caused by aggregation of same constant power loads in parallel connection', *International Journal of IET Generation, Transmission and Distribution*, Vol. 13, No. 13, pp.2637–2645.

Wu, Y. and Guerrero, J.M. and Wu, Y. (2019) 'Distributed coordination control for suppressing circulating current in parallel inverters of islanded microgrid', *International Journal of IET Generation, Transmission and Distribution*, Vol. 13, No. 7, pp.968–975.

Wu, Y., Barati, M. and Lim, G.J. (2006) 'A pool strategy of microgrid in power distribution electricity market', *International Journal of IEEE Transactions on Power Systems*, Vol. 35, No. 1, pp.3–12.

Yan, X., Cui, Y. and Cui, S. (2019) 'Control method of parallel inverters with self-synchronizing characteristics in distributed microgrid', *International Journal of Energies*, Vol. 12, No. 20, pp.3871–3890.

Yang, L., Hu, Z. and Xie, S. et al. (2019) 'Adjustable virtual inertia control of supercapacitors in PV-based AC microgrid cluster', *International Journal of Electric Power Systems Research*, Vol. 173, pp.71–85.

Zhang, L., Zheng, H. and Wan, T. et al. (2021) 'An integrated control algorithm of power distribution for islanded microgrid based on improved virtual synchronous generator', *International Journal of IET Renewable Power Generation*, Vol. 15, No. 12, pp.2674–2685.